Chen L et al. (2022) Mir-146a-3p Mediated Protection of Myocardial Cells by Suppressing Pparα in Diabetic Heart Failure: Impacts on Fitness Players and their Cardiovascular Fitness. Revista Internacional de Medicina y Ciencias de la Actividad Física y el Deporte vol. 22 (88.1) pp. 355-376.
DOI: https://doi.org/10.15366/rimcafd2022.88.1.025

ORIGINAL

Mir-146a-3p Mediated Protection of Myocardial Cells by Suppressing Pparα in Diabetic Heart Failure: Impacts on Fitness Players and their Cardiovascular Fitness

Jianxiang Gan[1], Mengyu Zhang[1], Liang Chen[1*]

[1] Department of Cardiovascular Medicine, Nanjing Hospital affiliated to Nanjing Medical University, Nanjing Medical University, Nanjing 210029, Jiangsu, China.
E-mail: 18795847883@163.com

Recibido 05 de junio de 2021 **Received** June 05, 2021
Aceptado 26 de junio de 2022 **Accepted** June 26, 2022

ABSTRACT

Background: Diabetic heart failure (DHF) poses a significant risk to cardiovascular health, particularly in individuals with diabetes, affecting their overall fitness and ability to engage in physical activities, including fitness players. The pathogenesis of DHF involves complex mechanisms such as cardiac hypertrophy, ventricular dilation, and compromised systolic function. This study aims to identify miRNAs related to DHF prognosis and unravel their molecular mechanisms in relation to DHF, with a specific focus on the implications for fitness players and their cardiovascular fitness. **Methods:** Public databases were searched for miRNA sequencing data from the peripheral blood of DHF patients, with further verification of expression levels conducted via qRT-PCR in patients' samples. Cellular proliferation was assessed using BrdU assays, while apoptosis, mitochondrial membrane potential (MMP), and reactive oxygen species (ROS) levels were evaluated through TUNEL staining and respective assays. Oxidative stress was measured by examining malondialdehyde (MDA) levels and superoxide dismutase (SOD) activity. Apoptosis-related markers were analyzed via Western blotting, and the interaction between miR-146a-3p and PPARα was confirmed through luciferase reporter assays. **Results:** Analysis of public datasets revealed a significant decrease in miR-146a-3p levels in DHF patients, correlating with patient survival rates. Overexpression of miR-146a-3p in high-glucose cultured H9C2 cells demonstrated its ability to bind and suppress PPARα, enhancing cellular proliferation and reducing apoptosis and oxidative stress. Furthermore, extracellular vehicles (EVs) loaded with miR-146a-3p showed potential in mitigating cardiac damage in DHF model rats,

suggesting a novel therapeutic strategy that could be particularly beneficial for fitness players seeking to maintain or improve cardiovascular fitness in the face of DHF. **Conclusions:** MiR-146a-3p plays a crucial role in regulating myocardial cell apoptosis and oxidative stress by targeting PPARα, offering a promising approach to alleviate cardiac damage induced by high glucose levels. For fitness players, especially those with diabetes, miR-146a-3p represents a potential molecular target to enhance cardiovascular fitness and mitigate the risks associated with DHF. Further research is needed to explore the therapeutic applications of miR-146a-3p in improving cardiovascular health and performance in athletic populations.

KEYWORDS: diabetic heart failure; miR-146a-3p; PPARα; apoptosis; oxidative stress; extracellular vehicles

1. INTRODUCTION

Diabetic heart failure (DHF) represents a critical intersection of metabolic and cardiovascular pathologies, constituting a significant challenge within the clinical landscape. As a specific manifestation of heart failure precipitated by the systemic metabolic aberrations characteristic of diabetes, DHF is distinguished by a unique pathophysiology that encompasses cardiac hypertrophy, ventricular dilation, and compromised systolic function. The intricate mechanisms underpinning the progression from diabetes to DHF involve an array of molecular and cellular processes, including but not limited to inflammation, oxidative stress, and metabolic dysregulation. Despite considerable advances in understanding diabetes-related cardiovascular complications, the specific molecular pathways contributing to the transition to DHF remain incompletely elucidated(Fukushima & Lopaschuk, 2016). The advent of microRNA (miRNA) research has opened new avenues for exploring the molecular underpinnings of diseases, offering insights into previously unrecognized regulatory mechanisms. miRNAs, short non-coding RNA molecules, have emerged as critical post-transcriptional regulators of gene expression, (Kannel, Hjortland, & Castelli, 1974) capable of modulating diverse biological processes implicated in both the onset and progression of various pathologies, including DHF. Among these, miR-146a-3p has attracted attention for its potential role in cardiovascular diseases(Dillmann, 2019; Jia, Hill, & Sowers, 2018; Rydén et al., 2000; Shindler et al., 1996), with preliminary evidence suggesting its involvement in modulating inflammatory responses and oxidative stress pathways, both of which are pivotal in the pathogenesis of DHF (ALSHAWY, Ibrahim, Hussein, & Lahlah, 2019; Cosmi et al., 2018). This study seeks to delve into the relationship between miR-146a-3p and DHF, with an emphasis on understanding how miR-146a-3p might influence the disease process through the suppression of peroxisome proliferator-activated receptor alpha (PPARα), a nuclear receptor involved in lipid metabolism and inflammation. The rationale for focusing on miR-146a-3p

stems from its observed downregulation in DHF patients and its potential as a therapeutic target for ameliorating heart failure symptoms and improving cardiac function(Jia, Whaley-Connell, & Sowers, 2018). Furthermore, given the increasing recognition of the importance of maintaining cardiovascular health for overall fitness, particularly in individuals with a high level of physical activity such as athletes, this study also aims to explore the implications of miR-146a-3p modulation for enhancing cardiovascular resilience and performance in this demographic. Athletes, especially those with or at risk of diabetes, may face unique challenges related to cardiovascular health, underscoring the need for targeted interventions that can support cardiac function and mitigate the risk of developing DHF(Akman, Cairns, Comar, & Hrozencik, 2014; Jaquenod De Giusti, Palomeque, & Mattiazzi, 2022). In this investigation is poised to contribute significantly to the existing body of knowledge on DHF by elucidating the protective role of miR-146a-3p against high-glucose-induced myocardial damage through the suppression of PPARα. By integrating molecular biology with clinical insights, this study aims to pave the way for novel therapeutic strategies that could benefit a wide range of patients, including those engaged in demanding physical activities, thereby enhancing their quality of life and athletic performance (Cheng et al., 2009; Das et al., 2012; Guo & Nair, 2017; Harada et al., 2014; Li, Fan, Chen, & Wang, 2020; Melman, Shah, & Das, 2014; Wong, Wang, Liew, Richards, & Chen, 2016).

2. Methods

2.1 Patients

A total of 63 DHF patients aged from 30 to 80 years and diagnosed with type II diabetes from Sep. 2018 to Apr. 2022 in Nanjing Hospital affiliated with Nanjing Medical University are recruited, and 47 age-matched healthy volunteers are also included in this study. All participants noticed the content of all experiments and signed the informed consent form.

In this study, the inclusion criteria are as follows: 1) type II diabetes history over 6 months; 2) cardiomyopathy; 3) diagnosis as heart failure according to the guidelines of the 2012 European Society of Cardiology for heart failure; 4) heart failure history over 6 months 5) left ventricular ejection fraction (LVEF) less than 50%. And the exclusion criteria are as follows: 1) pregnancy; 2) symptomatic macro vascular or microvascular disease; 3) myocardial infarction history; 4) other complications including tumor, immune disease, thyroid dysfunction, or other psychosis. The peripheral blood of patients and healthy people are collected and centrifuged to isolate serum.

2.2 Animals

The 16 weeks-old adult male Sprague–Dawley (SD) rats are

purchased from Cyagen Bioscience Co. Ltd (Suzhou, China), and maintained under the constant condition with controlled temperature (22-24°C) and a 12-12 hours' light-dark cycle, all rats are free to access food and water. The control group rats received normal rat chow (SWC9101, Xietong Bio, China), and the heart failure rat model is established by referring to previous studies. In brief, the rats received a high-fat diet (HFD) (70.5% normal rat chow, 16% lard,), 2.5% cholesterol, and 1% sodium cholate) (XTHF45, Xietong Bio, China) for 3 weeks and received intraperitoneal injections of streptozotocin (STZ) with a 30 mg/kg dose (Louch, Sheehan, & Wolska, 2011). All experiments are investigated and approved by the Ethics Committee of Nanjing Hospital affiliated with Nanjing Medical University.

2.3 Cell culture and transfection

H9C2 rat myocardial cells and rat bone mesenchymal stem cells (RBMSCs) are purchased from ATCC (CRL-1446, ATCC, USA) and Cyagen corporation (HUXMA-01001, Cyagen, China). H9C2 cells are cultured in Modified Eagle's medium (DMEM) (11965092, Gibco, USA) with 10% fetal bovine serum (FBS) (10100147, Gibco, USA) and 100 U/ml penicillin-streptomycin (Pen/Strep) (15140122, Gibco, USA). RBMSCs are cultured in the Minimum Essential Medium – Alpha Eagle (BE02-002F, Lonza, Switzerland) with 10% FBS, 100 U/ml Pen/Strep, and 10 U/mL heparin (H3149, Sigma, USA) (Zou et al., 2018). All cells are maintained in the constant temperature and humidity incubator in the 5% CO2 environment at 37 °C.

2.4 High glucose treatment

When the confluence reached 70%-80%, H9C2 cells are dissociated using 0.25% Trypsin-EDTA (25200072, Gibco, USA) and passaged to a 6-well plate. After 24 hours of culturing, D-glucose (G8644, Sigma, USA) solutions are added into the culture medium with 30 mM working concentration for high glucose treatment and keep cultured for 48 hours (Baglio et al., 2015).

2.5 Extracellular Vesicles extraction

The cultured HBMSCs are absorbed culture medium and washed with 1 X PBS to remove residual FBS, then added fresh culture medium with 10% Exosome-depleted FBS (A2720803, Gibco, USA). After 48 hours cultured, the supernatant culture medium is collected and extracted EVs through density gradient centrifugation method according to previously (Zhang et al., 2018).

2.6 qRT-PCR

Total RNA of peripheral blood and cells are extracted using miRNeasy serum/plasma kit (217184, Qiagen, Germany) and RNeasy Mini Kit (74104,

Qiagen, Germany) following the manufacturer's protocol. Then an equal amount of mRNAs is reverse transcribed using Mir-X miRNA First-Strand Synthesis Kit (638315, Takara, Japan) with specific stem-loop primers. qRT-PCRs are performed with TB Green® Premix Ex Taq™ II (Tli RNaseH Plus) (RR820Q, Takara, Japan) and detected through CFX Opus 96 Real-Time PCR System (12011319, Bio-Rad, USA). The Ct values of miRNAs are recorded and calculated for relative expression levels through the $2^{-\Delta\Delta Ct}$ method according to Rnu6 (U6) gene level.

2.7 Western blotting

Cells and tissues proteins are lysed using RIPA buffer (P0013C, Beyotime, China) with a Protein inhibitor cocktail (P1005, Beyotime, China), and the concentrations are quantified through a BCA protein assay kit (P0011, Beyotime, China). The protein lysis is denatured with 5X SDS loading (P0015, Beyotime, China) at 95℃ for 10 min. For western blotting, the boiled total proteins are electrophoresed in 10% Tris-Glycine Precast gel (PG01210-S, Solarbio, China) and transferred to the Immobilon-NC membrane (HATF00010, Millipore, USA) then blocked with 5% non-fat milk (P0216-300g, Beyo time, China) in PBS. The NC membrane is fertilized with primary antibodies in 3% BSA (ST023-50g, Beyotime, China) solution overnight, then incubated with HRP-conjugated second antibodies for 1 hour on the second day.

The membrane is developed with Immobilon Western HRP Substrate ECL kit (WBKLS0500, Millipore, USA) and detected using Chemi Doc XRS+ System (1708265, Bio-Rad, USA), the grey values of protein bands are quantified using Image J software (Ver 1.53n). The primary antibodies used in this study are as follows: Bcl-2 (1:2000) (ab182858, Abcam, UK), Bax (1:5000) (ab32503, Abcam, UK), Cleaved Caspase-3 (1:1000) (9661S, Cell Signaling, USA), Caspase-3 (1:1000) (9662S, Cell Signaling, USA), PPARα (1:1000) (15540-1-AP, Proteintch, USA), NOX1 (ab131088, Abcam, UK), SOD1 (1:1000) (37385S, Cell Signaling, USA), GAPDH (1:50000) (BM1623, BOSTER, China), β-actin (1:20000) (BM3873, BOSTER, China).

2.8 BrdU and TUNEL assay

H9C2 cells are seeded into a 6-well plate and cultured for at least one day. After treatment, the BrdU solution (B8010, Solarbio, China) is added to the culture medium to reach a 10 μM working concentration and incubated for 24 hours. And the cellular apoptosis levels are detected by Cell Meter TUNEL Apoptosis Assay Kit (T2130, Solarbio, China) following the manufacturer's protocol. The BrdU- or TUNEL- positive cells are detected and captured by ZEISS Axioscope 5 system, and the fluorescent images are analyzed to count the number of positive cells using ImageJ software.

2.9 Mitochondria membrane potential (MMP)

The cellular mitochondria membrane potentials are detected by Rhodamine 123 (R8030, Solarbio, China) staining. Briefly, the Rhodamine 123 solution is added into culture medium to reach the 10 μM final working concentration and fertilized at 37℃ for 1 hour. After fixing the cells with 4% PFA solution overnight the cell samples are washed with 1 X PBS, and cellular mitochondria membrane potentials levels are captured by ZEISS Axioscope 5 system at and quantified by the intensities of fluorescent.

2.10 Reactive oxygen species (ROS) levels detection

The cellular ROS levels are explored using the Reactive Oxygen Species Assay Kit (CA1410, Solarbio, China) according to the manufacturer's recommended protocol. Briefly, the treated cells in a 96-well plate are changed the culture medium to the 1 mL 2′,7′-dichlorofluorescein diacetate (DCFH-DA) probe diluted in serum-free culture medium (1:1000) and incubated at 37℃ for 20 min. Then wash the cell using the serum-free culture medium three times and measured the fluorescent intensities through the BioTek Synergy H1 Plate Reader (BioTek, USA) at 525nm.

2.11 Cellular oxidative stress detection

Cellular oxidative stress levels are determined by malondialdehyde (MDA) levels assay and superoxide dismutase (SOD) activity assay. We use the MDA content detection kit (BC0020, Solarbio, China) and SOD activity detection kit (BC0170, Solarbio, China) following the manufacturer's protocol. The OD values of samples are detected at 532nm and 600nm for MDA levels, and 560 nm for SOD levels using BioTek Synergy H1 Plate Reader.

2.12 Dual luciferase reporter assay

The wild-type and mutant 3'UTR region of PPARα is subcloned into pGL3 reporter Vector using KpnI and XhoI enzyme sites to construct PPARα-3'UTR plasmid and PPARα-3'UTR Mutant plasmid. The two plasmids are co-transfected with miR-146a-3p mimic or control mimic into H9C2 cells using Lipofectamine 3000 according to manufacturer's protocol. After 48 hours of transfection, the luciferase activities are detected using the Dual Luciferase Reporter Gene Assay kit (11402ES60, YEASEN, China).

2.13 HE staining

The rats are anesthesia using isoflurane and perfused with pre-cold 0.9% saline followed by 4% PFA, then fix the heart tissues with 4% PFA overnight. After dehydrated with 30% sucrose solution, the tissues are embedded in paraffin and section into 0.4 μM slices. Next, the slices are

deparaffinized and stained with hematoxylin (G1120, Solarbio, China) for 10 min, differentiated with hydrochloric acid ethanol mixture for 60s and washed by water two times. Then stain the slices in eosin solution for 1 min and quickly dehydrated by gradient ethanol solution and transparent with xylene, mounting the slice with neutral balsam (G8590, Solarbio, China) and observing under the microscope.

2.14 Bioinformatics analysis

The public datasets GSE196656, GSE179105, and GSE109051 are downloaded for analysis (Abu-Halima, Meese, Abdul-Khaliq, & Raedle-Hurst, 2021; Luo et al., 2021; Wang et al., 2022). The miRNA counts are quantified using Salmon software (Ver 1.7.0) (Shah et al., 2018) and the differential expression genes (DEGs) are explored by the DEseq2 package (Ver 3.16) (Patro, Duggal, Love, Irizarry, & Kingsford, 2017). The heatmaps and Veen plots are plotted using pheatmap (Ver 1.0.12) and Veen (Ver 1.11) packages. All bioinformatic analyses are performed at R (Ver 4.1.0) in RStudio (Ver 2021.09.1).

2.15 Statistical analysis

Statistical analyses are analyzed using Prism software (Ver 7.0). The differences between the two groups are analyzed through the Student's t-test or Mann–Whitney U test method. The differences between multiple groups were analyzed by one-way ANOVA followed by the Tukey test. All experiments are repeated at least three times, and the $p < 0.05$ indicates a statical significant difference.

3. Results

3.1 Peripheral blood miR-146a-3p is correlated with the prognosis of diabetic heart failure

To explore the potential relationship between miRNAs and the prognosis of DHF patients, we search the public database and analyze RNA-seq data. After searching the data about peripheral miRNAs sequencing of DHF patients in the GEO database, we find GSE196656, GSE179105 and GSE109051 met our criteria. Through DEG analysis, the miR-548ar-3p, miR-142-3p, miR-36-5p, miR-146a-3p, and miR-130e-5p show significant down-regulated in the peripheral blood of DHF patients (Fig 1. A-B). Meanwhile, we verify the alternation of these miRNAs in the peripheral blood samples of in-hospital DHF patients. Compared to the control group, the qRT-PCR results show miR-548ar-3p, miR-142-3p and miR-36-5p are slightly decreased ($p < 0.05$), miR-30e-5p shows not significantly changed ($p > 0.05$), and miR-146a-3p is greatly decreased ($p < 0.001$) in DHF group (Fig. 1C), therefore we focus on the miR-146a-3p in the following study. After surgical treatment, the

blood miR-146a-3p is notably increased ($p < 0.001$) compared to pre-treatment in DHF patients (Fig. 1D). The survival rate analysis results also show miR-146a-3p highly expressed patients DHF present better survival rates, and miR-146a-3p lowly expressed DNF patients present worse survival rates (Fig. 1E). The above results hint that miR-146a-3p is down-regulated and correlated with survival rate in DHF patients.

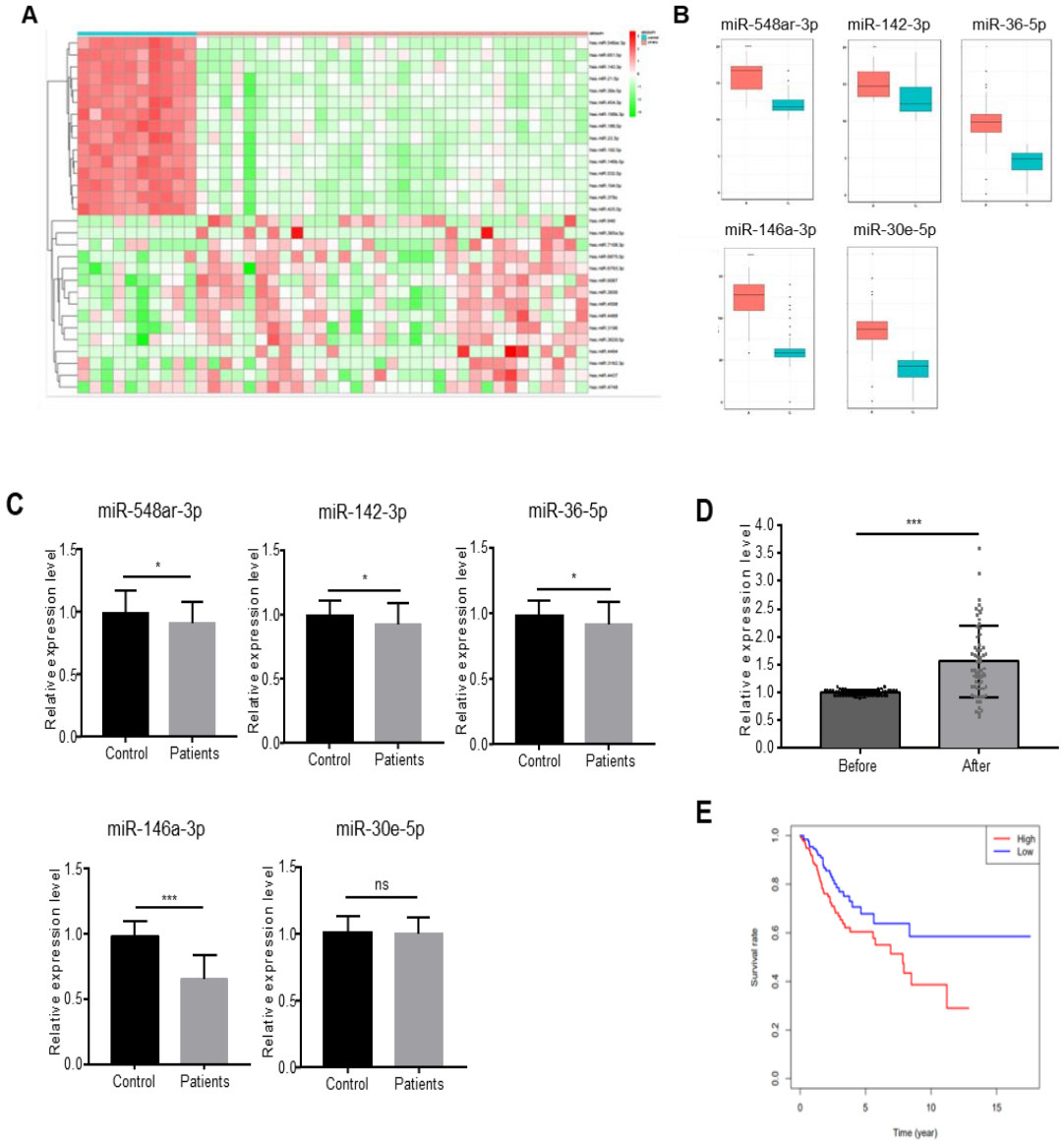

Figure 1: The miR-146a-3p is down-regulated in the peripheral blood of DHF patients. A) The heat map of TOP30 differential expression miRNAs. B) The five miRNAs expression levels in the peripheral blood of control and patients in public GEO datasets. C) The qRT-PCR results of the five miRNAs expression levels in healthy people and diabetic heart failure patients. D) The comparison of peripheral blood miR-146a-3p expression levels in the patients before and after treatment. E) The survival analysis of DHF patients with low or high miR-146a-3p expression. * indicates p <0.05, *** indicates p <0.001, and ns indicates not significant. The error bar presents as mean values ± SEM. All experiments are repeated at least three times.

3.2 Overexpressed miR-146a-3p alleviates high glucose-induced cellular damage

To explore the function of miR-146a-3p in the DHF, we culture the H9c2 cells, a rat myocardial cell line, on the high glucose (HG) environment to construct an in-vitro HFD model. Then we transfect the control mimic or miR-146a-3p mimic in the HG environment, qRT-PCR results show the miR-146a-3p is significantly elevated in the miR-146a-3p mimic group compared to the control group ($p < 0.001$), HG group ($p < 0.001$), and control mimic group ($p < 0.001$) (Fig. 2A). Next, we detect the effects of miR-146a-3p on cellular proliferation and survival through BrdU staining and TUNEL assay.

The results indicate high glucose treatment reduces cell proliferation ($p < 0.01$) and enhance apoptosis ($p < 0.01$), and overexpressed miR-146a-3p mimic could significantly increase $BrdU^+$ proliferative cells ($p < 0.001$) and decreased $TUNEL^+$ apoptotic cells ($p < 0.001$) compared to control mimic group (Fig. 2B-C). The western blot results show apoptosis-related proteins including Bax ($p < 0.01$) and cleaved caspase-3 ($p < 0.001$) levels are up-regulated, and Bcl-2 ($p < 0.001$) level is down-regulated after miR-146a-3p overexpression in HG environment (Fig. 2D-E).

Next, we detect the mitochondrial functions in different groups, and the results show overexpressed miR-146a-3p could significantly elevate MMP levels ($p < 0.001$) in HG-treated cells (Fig. 2F and 2H). The HG treatment usually induces excess oxidative stress and impairs cellular functions, we find overexpressed miR-146a-3p could mildly increase cellular ROS levels ($p < 0.05$) (Fig. 2G and 2I), and greatly alleviate MDA ($p < 0.01$) and SOD levels ($p < 0.001$) (Fig. 2J-K). Thus, these results indicate that miR-146a-3p could reduce cellular apoptosis and enhance proliferation, and relieve the mitochondrial damage levels and oxidative stress levels in HG-treated H9c2 cells.

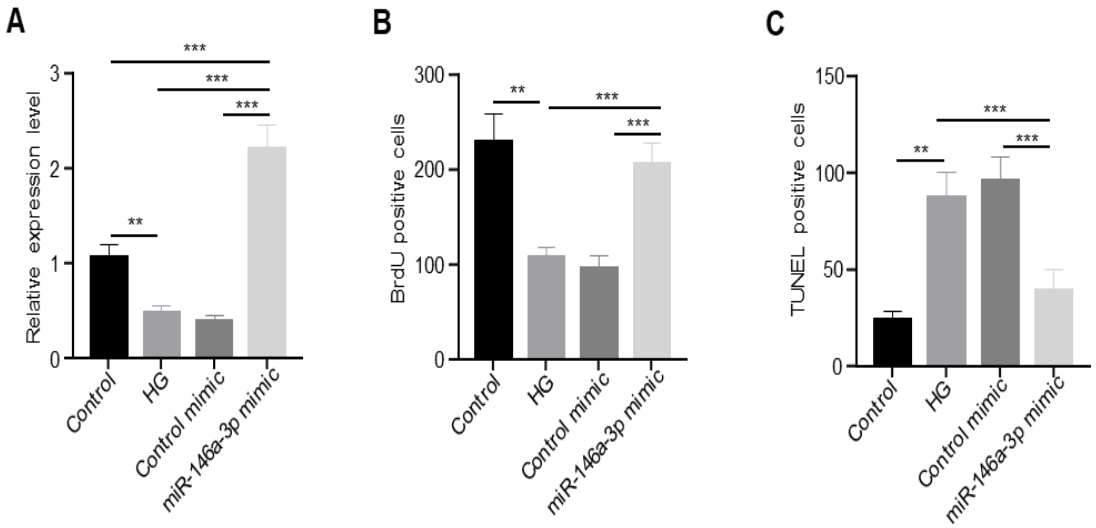

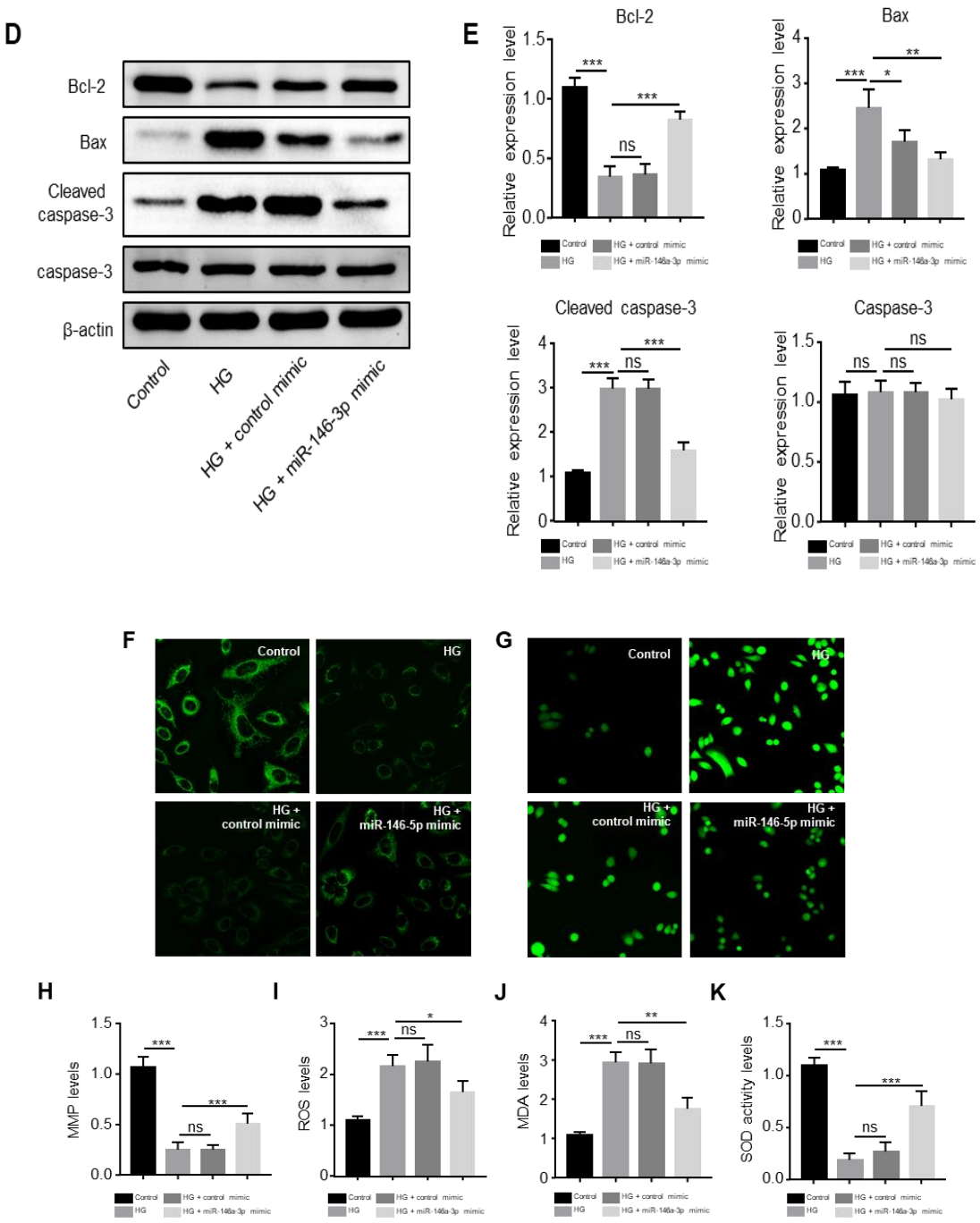

Figure 2: The miR-146a-3p could alleviate high glucose-induced cellular damage in H9c2 cells. A) The miR-146a-3p expression level in the cells of different groups. B) The number of BrdU-positive cells in different groups. C)The number of TUNEL-positive cells in different groups. D-E) Western blot detected apoptosis-related proteins including Bcl-2, Bax, Cleaved Caspase-3, and Caspase-3 expressions in different groups. F) The cellular MMP staining in different groups. G) The DCFHDA probe staining shows the ROS levels in different groups. H) The histology of MMP levels in each group. I) The histology of ROS levels in each group. J) The histology of MDA levels in each group. K) The histology of SOD activity levels in each group. * indicates p <0.05, ** indicates p <0.01, *** indicates p <0.001, and ns indicates not significant. The error bar presents as mean values ± SEM. All experiments are repeated at least three times.

3.3 miR-146a-3p could bind PPARα and regulate its expression

To explore the potential mechanism of miR-146a-3p to alleviate high glucose-induced cellular damage, we analyze the bulk-mRNA sequencing datasets GSE26887 of DHF patients, then filter all DEGs with $\log_2$|Fold Change| >2 and $p < 0.01$. When intersecting the filtered DGEs with potential miR-146a-3p targeted genes predicted by the miRBase website, we find PPARα, SIRT1, and IL-8 are up-regulated in DHF patients' blood (Fig. 3A).

The ELISA data show PPARα is up-regulated ($p < 0.001$), but SIRT1 ($p > 0.05$) and IL-8 ($p > 0.05$) are not significantly changed in peripheral blood between control and DHF patients (Fig. 3B). Therefore, we speculate that miR-146a-3p may regulate the expression of PPARα in DHF disease.

To prove this hypothesis, we clone the 3'UTR region of PPARα into the pcDNA3.1 luciferase reporter vector to construct the PPARα-3'UTR plasmid and PPARα-3'UTR-Mutant plasmid. Then we co-transfect these two PPARα reporter plasmids with control mimic or miR-146a-3p mimic into H9c2 cells and detect the luciferase activities.

The fluorescent intensity of miR-146a-3p mimic + PPARα-3'UTR group is lower than the control mimic + PPARα-3'UTR group ($p < 0.001$), and the intensities show no significant difference between miR-146a-3p + PPARα-3'UTR-Mutant group and control mimic + PPARα-3'UTR-Mutant group ($p > 0.05$) (Fig. 3C-D). Meanwhile, we respectively transfect the control mimic, miR-146a-3p mimic, and miR-146a-3p antagonist into H9c2 cells in the high glucose environment, qRT-PCR results show the miR-146a-3p is significantly elevated in the miR-146a-3p mimic group ($p < 0.01$) and decreased in miR-146a-3p antagonist group ($p < 0.01$).

PPARα shows a ~60% decrease after miR-146a-3p overexpression, and about a two-fold increase after the miR-146a-3p knockdown (Fig 3. F-G). Hence, these data show miR-146a-3p could directly bind the 3'UTR region of PPARα and suppress its expression in H9c2 cells.

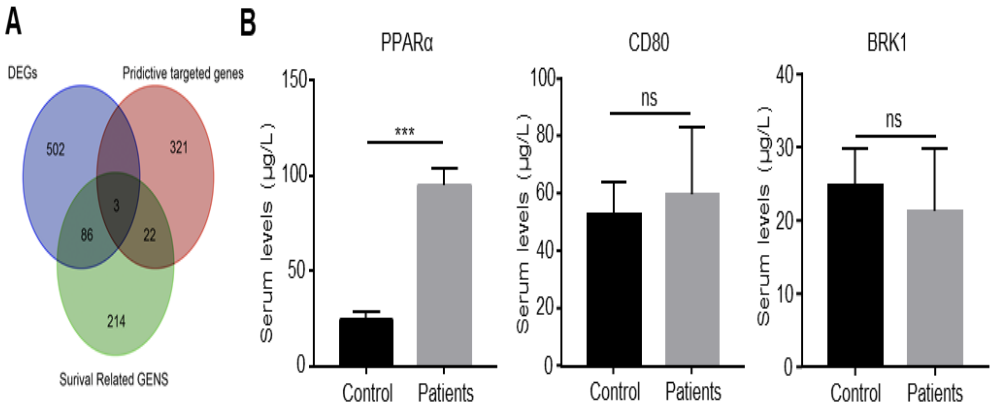

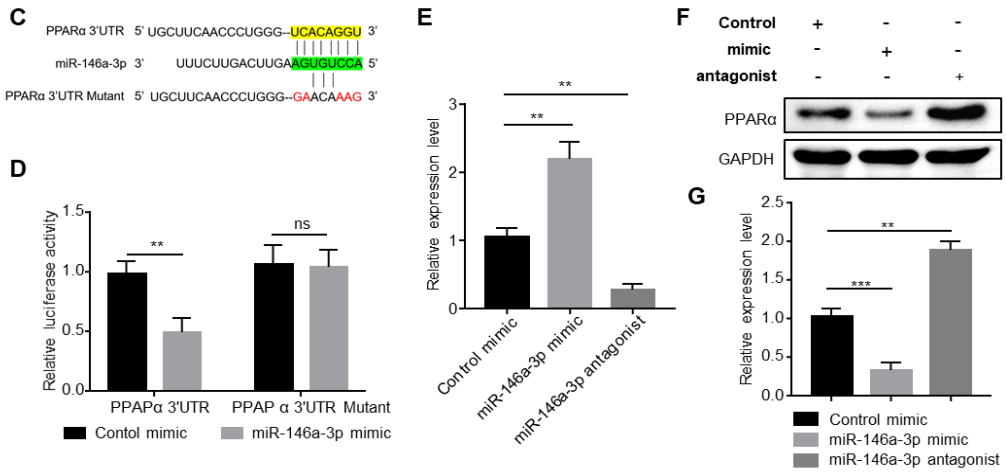

Figure 3: miR-146a-3p could bind and regulate PPARα in H9c2 cells. A) The Veen diagram of the DEGs set, DHF patients' survival-related genes set and miR-146a-3p predict target genes set. B) The ELISA results of PPARα, CD80, and BRK1 in the peripheral blood of DHF patients and the control group. C) The predictive target sequences of miR-146a-3p binding with the 3'UTR region of PPARα, and the mutant site of constructed PPARα-3'UTR-Mutant plasmids. Yellow and green bases indicate the binding sites of PPARα-3'UTR and miR-146a-3p respectively, and red bases indicate mutant sites of the PPARα-3'UTR region in constructed plasmids. D) The luciferase activities result in each group. E) The miR-146a-3p expression levels in H9c2 cells of three groups are detected by qRT-PCR. F-G) The PPARα protein levels in three groups. ** indicates p <0.01, *** indicates p <0.001, and ns indicates not significant. The error bar presents as mean values ± SEM. All experiments are repeated at least three times.

3.4 miR-146a-3p could alleviate myocardial cells injury through PPARα

Based on the above results, we speculate that miR-146a-3p may protect the myocardial cells in the high-glucose environment by inhibiting PPARα expression. To verify this hypothesis, we co-transfect miR-146a-3p mimic with GFP or PPARα overexpression plasmids into H9c2 cells. The miR-146a-3p levels in the two groups show no significant difference (p > 0.05) (Fig. 4A), and the PPARα is greatly increased (p < 0.01) in the miR-146a-3p + PPARα group than miR-146a-3p + GFP (Fig. 4B).

The apoptosis-related proteins Bax (p < 0.05) and cleaved-capsease3 levels (p < 0.01) are elevated, and Bcl-2 level (p < 0.05) is reduced in miR-146a-3p + PPARα group compared to miR-146a-3p + GFP group (Fig. 4B). The staining results show $BrdU^+$ cells number is decreased (p < 0.01) but $TUNEL^+$ cells number is increased (p < 0.01) after PPARα overexpression (Fig. 4C-D). Also, the cellular MMP level (p < 0.001) (Fig. 4E) and MDA level (p < 0.01) (Fig. 4G) are decreased, and ROS level (p < 0.01) (Fig. 4F) and SOD level (p < 0.01) (Fig. 4H) are increased in miR-146a-3p + PPARα group. These results indicate overexpressed PPARα could reverse the protective function induced by miR-146a-3p in H9c2 cells. Otherwise, miR-146a-3p

protects myocardial cells in the high glucose environment by suppressing PPARα overexpression.

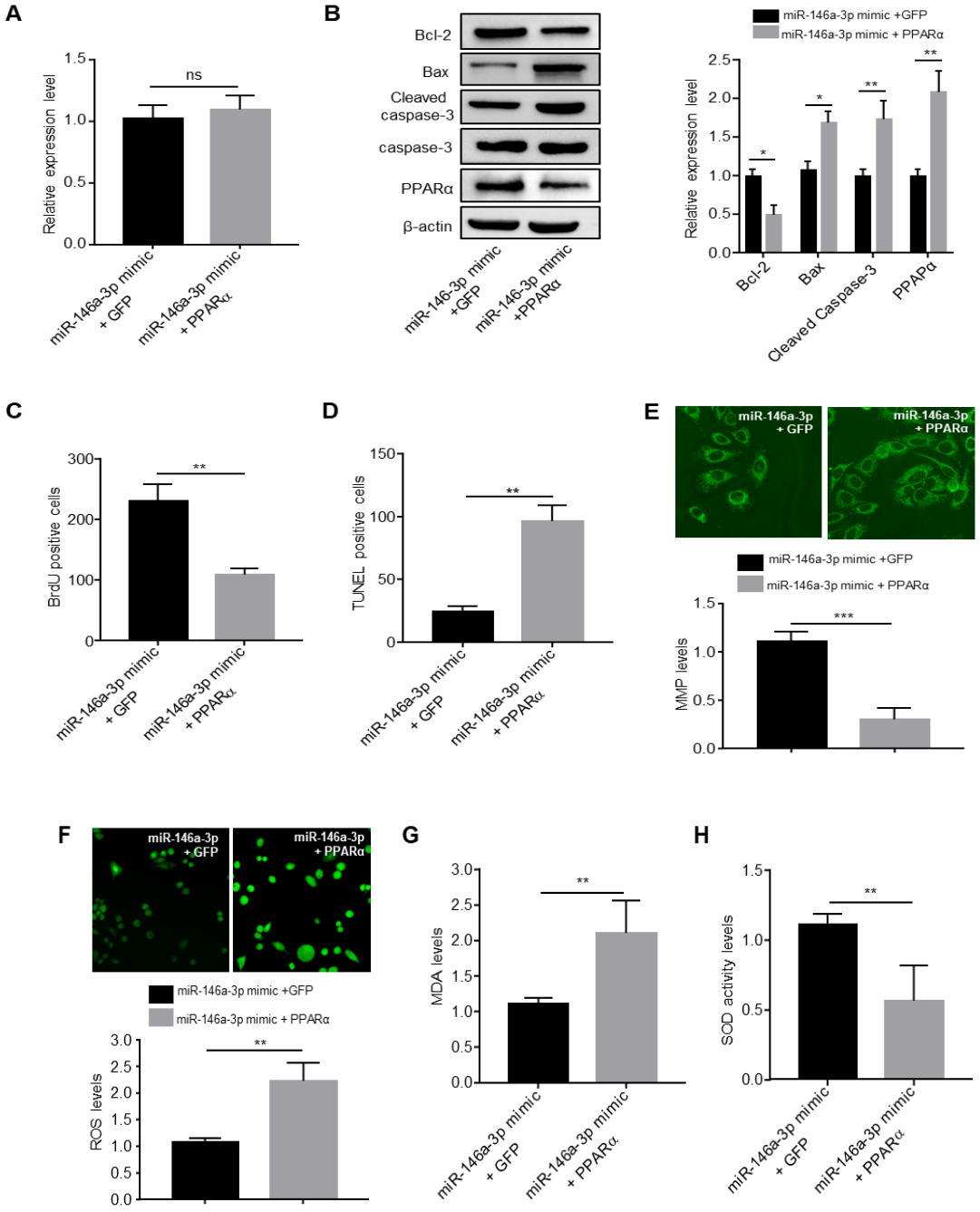

Figure 4. miR-146a-3p reduces high-glucose induced cellular damage by inhibiting PPARα in H9c2 cells. A) The miR-146a-3p expression levels in two groups. B) PPARα and apoptosis-related protein expression levels in two groups. C) The BrdU positive cell number in two groups. D) The TUNEL positive cell number in two groups. E) The MMP levels in different cellular groups. F) The ROS levels in different cellular groups. G) The histology of MDA levels in two groups. H) The histology of SOD activity levels in two groups. * indicates p <0.05, ** indicates p <0.01, *** indicates p <0.001, and ns indicates not significant. The error bar presents as mean values ± SEM. All experiments are repeated at least three times.

3.5 Exosomes packaged with miR-146a-3p could reduce myocardial damage in rat

The above *in vivo* studies declare the protective function of miR-146a-3p in HG-treated myocardial cells, thus we try to test whether miR-146a-3p could alleviate heart failure in the STZ-induced T2DM rat model. Firstly, we overexpress the miR-146a-3p mimic or control mimic in rat bone marrow mesenchymal stem cells (RAMSCs) and extract the supernatant extracellular exosomes (EVs) of the culture medium after 48h of transfected. qRT-PCR results show the miR-146a-3p levels are greatly higher in miR-146a-3p mimic transfected EVs than control-mimic EVs ($p < 0.01$) (Fig. 5A). Next, we inject the purified EVs into STZ-induced T2DM model rats by caudal vein injection. After 21 days of injection, we find the miR-146a-3p-EVs group shows an increased miR-146a-3p level ($p < 0.001$) and reduced PPARα expression ($p < 0.05$) in the heart tissues compared to the control-EVs group (Fig. 5B-C). The TUNEL staining results hint the number of apoptosis cells is decreased ($p < 0.01$) after miR-146a-3p mimic EVs injection (Fig. 5D). The HE staining results indicate the control-EVs group mice present mildly fractured and disordered myocardial fiber, wide intercellular space, and nucleolysis of cardiac muscle cells in heat tissues, but miR-146a-3p-EVs group mice present more relative clear and regular cardiac muscle fibers (Fig. 5E). The weight ($p < 0.05$) and blood biochemical markers including blood glucose ($p < 0.001$), cholesterol ($p < 0.01$), and triacylglycerol levels ($p < 0.001$) of the miR-146a-3p-EVs group are all decreased after injection compared to the control-EVs group (Fig. 5F). Moreover, the mRNA levels of cardiac stress-related biomarkers including atrial natriuretic peptide (ANP) ($p < 0.001$), Brain natriuretic peptide (BNP) ($p < 0.001$), and myocardial fibrosis related maker Transforming growth factor beta 1 (TGF-β1) levels ($p < 0.01$) are down-regulated in the heart tissues of miR-146a-3p-EVs group mice. Similarly, the western blots show that NOX1 ($p < 0.01$) is down-regulated and SOD1 ($p < 0.05$) is up-regulated in the miR-146a-3p-EVs group. Thus, we conclude that tail vein injection with EVs packaged miR-146a-3p could greatly reduce PPARα levels in heart tissues and then alleviate the cardiac damage in STZ-induced T2DM rats.

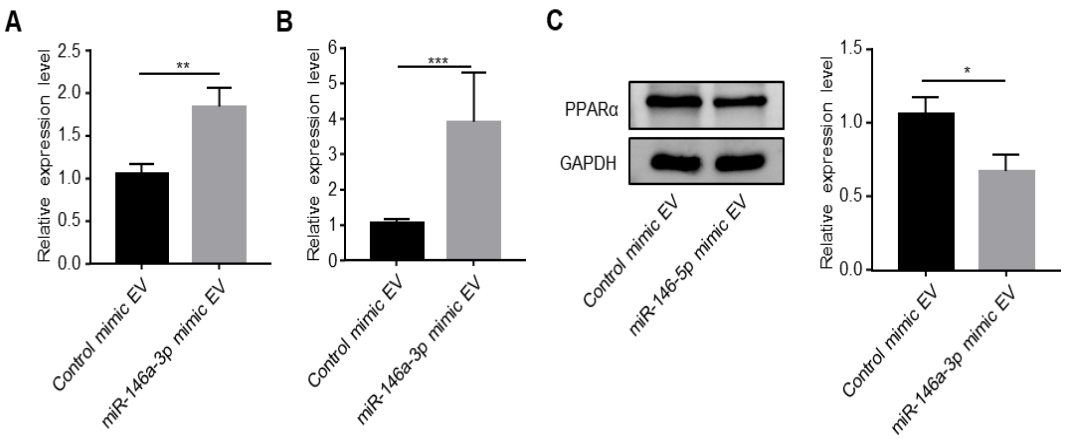

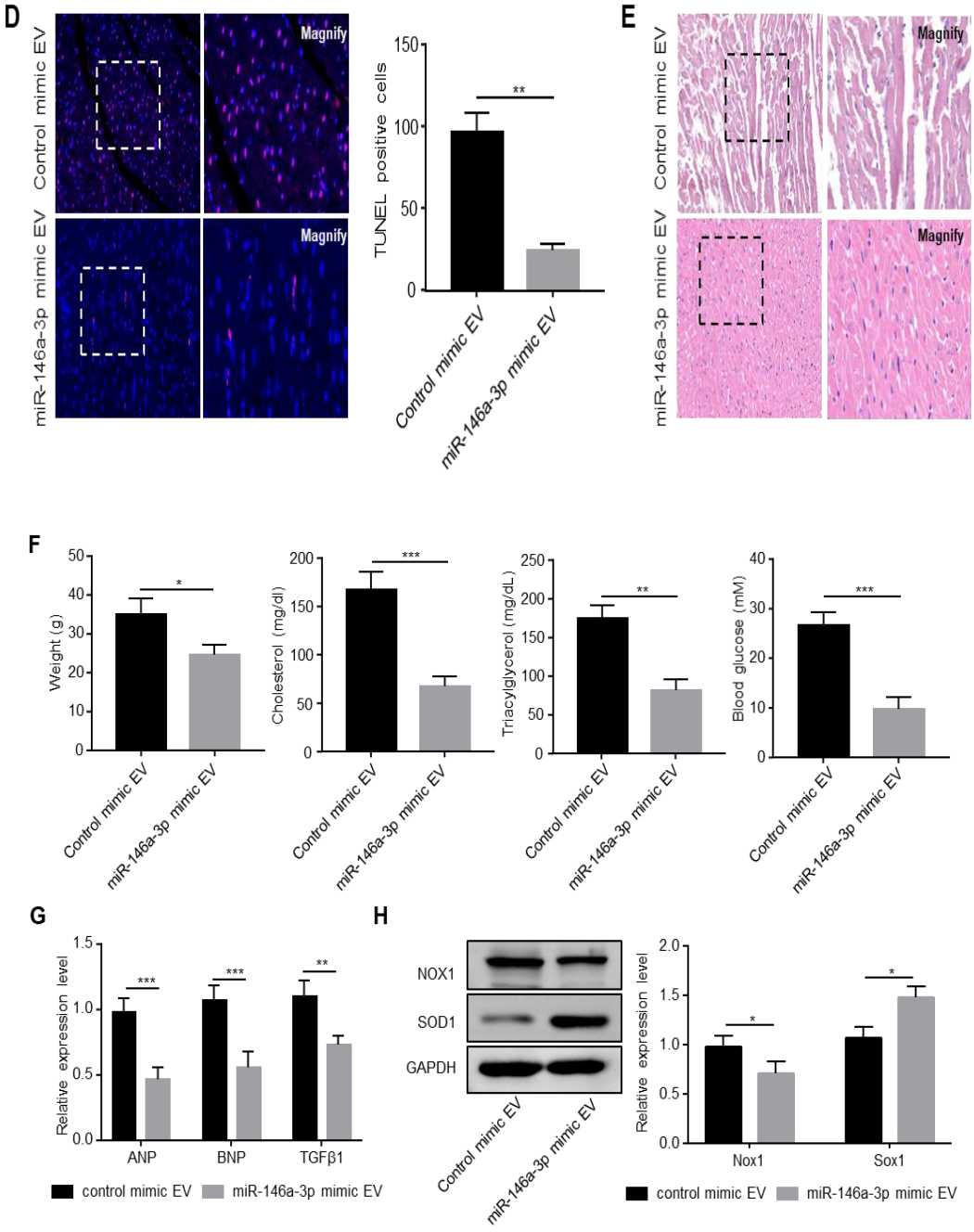

Figure 5: EVs packaged miR-146a-3p alleviate heart damage in HFD mice. A) The miR-146a-3p expression levels in the supernatant culture medium of two groups. B) The miR-146a-3p levels in the extracted EVs of two groups. C) The PPARα protein levels in heart tissues of two EVs injected groups. D) TUNEL staining results of the heart tissue sections in two groups. E) HE staining results of the heart tissues in two groups. F) Weight and blood biochemical indexes including cholesterol, triacylglycerol, and blood glucose comparison of two groups. G) The mRNA levels of myocardial fibrosis-related proteins including ANP, BNP, and TGF-β1 in each group after injection. H) The cardiac injury-related markers Nox1 and Sox1 expression levels in heart tissues of two groups. * indicates p <0.05, ** indicates p <0.01, and *** indicates p <0.001. The error bar presents as mean values ± SEM. All experiments are repeated at least three times.

4. Discussion

In this study, we firstly analysis the public DHF-related RNA-seq data and filter the significantly changed miRNAs in DHF patients' blood. Then verified the miR-146a-3p is greatly decreased in the clinical patients' blood samples and shows a closed correlated with the survival rate of patients. Actually, recent articles report the relationship between miR-146a in diverse cardiovascular diseases (CVDs). For example, sunitinib is a tyrosine kinase inhibitor and could induce cardiac dysfunction-related side effects, miR-146a is significantly down-regulated in the myocardium tissues of sunitinib-treated mice and related with 20% decreased left ventricle ejection fraction (LVEF) (Shen et al., 2019). In the doxorubicin (DOX) induced mice model overexpressed miR-146a could inhibit cellular apoptosis and enhance autophagy then alleviate cardiotoxicity induced by DOX (Pan et al., 2019).

Moreover, cardiomyocyte-specific miR-146a knockout mice present more severe myocardial infarction and cardiac dysfunction after ischemic reperfusion (I/R) treatment (Su et al., 2021). Moreover, several clinical studies show the SNP mutation of miR-146a rs2910164 would lead to a high risk of coronary heart disease (CHD) (Bao et al., 2022). However, the role of miR-146a in CVDs is still full of debatable. *Ming et al.* report miR-146a is increased in the 3 months and 30 months aged mice after myocardial infarction (MI), and *Junjue et al.* find an injection of miR-146a antagonist could attenuate cardiac impairment including increased LV end-diastolic pressure (LVEDP) and LV ±dp/dtmax (He, Lu, Song, Gong, & Li, 2019). And a 50 young acute ST-elevation myocardial infarction (STEMI) patients study indicates high expression of plasmatic miR-146a is closely correlated with major adverse cardiac events and predicts to worse prognosis and survival rate (Scărlătescu et al., 2022). The contradiction of miR-146a role in CVDs could be due to the complex functions of miR-146a, furthermore the miR-146a-5p and miR-146-3p may play different roles in disease, and past studies usually ignore this point. In this study, we find miR-146a-3p is significantly decreased in the DHF patients, and a lower level of miR-146a-3p in peripheral blood is related to a better survival rate in patients (Emad, 2018).

The miR-146a is shown protective roles in multiple CVDs through diverse pathways, such as the P53 pathway, IKK/ NF-κB signaling and p65/ NF-κB pathway (Gong et al., 2022; Pan et al., 2019; Xiong et al., 2022). Based on our results, we find miR-146a-3p could bind the 3'UTR region of PPARα, a nutritional sensor that regulated fatty acid and glucose catabolism, lipogenesis, and ketone body synthesis (Hashimoto et al., 2000; Xu et al., 2002). PPARα is highly expressed in the heart tissues and plays a very important role in heart development and function. As a transcription factor, PPARα regulates the cardiac metabolism switch from primarily consuming fatty acids to uptake glucose, ketone bodies, lactate, or fatty acid during

neonatal heart development (Madrazo & Kelly, 2008; Pol, Lieu, & Drosatos, 2015). In the adult healthy heart, PPARα deficiency would lead to disrupted fatty acids transport, glucose metabolism, and mitochondrial oxidation, then change the cardiac metabolism pattern which may lead to a lower and insufficient energy supply and lethal cardiomyopathy (Campbell et al., 2002; Haemmerle et al., 2011; Luptak et al., 2005; Watanabe et al., 2000). Multiple studies prove that cardiac specifically overexpressed PPARα could promote an imbalance of fatty acid uptake and fatty acid oxidative, aggravate mitochondrial lipid accumulation then cause diabetic cardiomyopathy phenotype (Cardoso et al., 2020; Jia, Hill, et al., 2018; Montaigne et al., 2014). The related results show miR-146a-3p could efficiently suppress cardiac PPARα expression levels and decreased cellular oxidative stress and mitochondrial impairments, then alleviate diabetes mellitus-induced heart failure. Furthermore, we overexpress the miR-146a-3p mimic in the RAMSCs and then inject the extracted EVs into STZ-induced T2DM rats to validate the protective function of miR-146a-3p *in-vivo*. Actually, Milano et al. report the injection of miR-146a-5p enriched EVs derived by human cardiac-resident mesenchymal progenitor cells (CPCs) could reduce cardiac cellular ROS levels in doxorubicin (DOX) and trastuzumab (Trz) co-induced cardiotoxicity rats (Milano et al., 2020). In our study, we find the EVs packaged miR-146-3p could significantly decrease cellular apoptosis and oxidative stress levels, reduce blood glucose/ cholesterol/triacylglycerol levels, and alleviate diabetes-induced cardiac dagame, which suggests the consistency of the protective function of miR-146a in cardiac disease.

5. Conclusion

This study illuminates the pivotal role of miR-146a-3p in modulating the pathophysiological mechanisms underlying diabetic heart failure (DHF), with significant implications for the cardiovascular health and fitness of individuals, particularly those engaged in athletic activities. Our findings demonstrate that the downregulation of miR-146a-3p in the peripheral blood of DHF patients correlates with adverse clinical outcomes, underscoring its potential as a biomarker for DHF prognosis. Crucially, the ability of miR-146a-3p to bind and suppress PPARα expression emerges as a key molecular mechanism through which it exerts protective effects against myocardial cell apoptosis and oxidative stress, thereby mitigating high-glucose-induced cardiac damage.

For fitness players, particularly those with underlying diabetic conditions, these findings offer a beacon of hope. The therapeutic modulation of miR-146a-3p levels presents a novel avenue to enhance myocardial resilience, improve cardiovascular fitness, and potentially extend the capacity for physical performance despite the challenges posed by DHF. The use of extracellular vehicles (EVs) to deliver miR-146a-3p directly to the myocardium exemplifies an innovative strategy that could be harnessed to safeguard the

hearts of those at heightened risk of DHF, enabling athletes to maintain rigorous training regimes without compromising their heart health. Moreover, this study contributes to the broader understanding of miRNA-mediated regulation in cardiovascular diseases, highlighting the intricate interplay between metabolic disorders and cardiac dysfunction. The insights gained here underscore the importance of integrating molecular biology with clinical strategies to combat the multifaceted impact of diabetes on the heart.

In conclusion, miR-146a-3p offers a promising target for therapeutic intervention in DHF, with the potential to significantly influence the management of cardiovascular health in diabetic patients, including those engaged in high-level physical activities. Future research should focus on translating these findings into clinical applications, exploring the efficacy of miR-146a-3p-based therapies in human trials, and further elucidating the molecular pathways through which miR-146a-3p and PPARα interact, to fully harness the potential of miR-146a-3p in improving the lives of those affected by diabetic heart failure.

Conflict of Interest Statement

In this study, the authors have no conflicts of interest to declare.

Funding Sources

There is no funding supported in this study.

Data Availability Statement

The public miRNA sequencing data of GEO datasets are openly and available in the NCBI GEO database, the detailed link of each GEO dataset used in this study is as follows: GSE196656, https://www.ncbi.nlm.nih.gov/geo/query/acc.cgi?acc=GSE196656; GSE179105, https://www.ncbi.nlm.nih.gov/geo/query/acc.cgi?acc=GSE179105; GSE179105, https://www.ncbi.nlm.nih.gov/geo/query/acc.cgi?acc=GSE109051.

All other data generated or analyzed during this study are included in this article. Further inquiries can be directed to the corresponding author.

Reference

Abu-Halima, M., Meese, E., Abdul-Khaliq, H., & Raedle-Hurst, T. (2021). MicroRNA-183-3p is a predictor of worsening heart failure in adult patients with transposition of the great arteries and a systemic right ventricle. *Frontiers in Cardiovascular Medicine, 8*, 730364.

Akman, O., Cairns, D., Comar, T. D., & Hrozencik, D. (2014). Integrated pest

management with a mixed birth rate for prey species. *Letters in Biomathematics, 1*(1), 87-95. doi:https://doi.org/10.30707/LiB1.1Akman

ALSHAWY, F. A., Ibrahim, A., Hussein, C., & Lahlah, M. (2019). First record of arrow bulleye, Priacanthus sagittarius Starnes, 1988 from the Syrian marine waters (Eastern Mediterranean). *FishTaxa, 4*(2), 21-24.

Baglio, S. R., Rooijers, K., Koppers-Lalic, D., Verweij, F. J., Pérez Lanzón, M., Zini, N., . . . Baldini, N. (2015). Human bone marrow-and adipose-mesenchymal stem cells secrete exosomes enriched in distinctive miRNA and tRNA species. *Stem cell research & therapy, 6*(1), 1-20.

Bao, Q., Li, R., Wang, C., Wang, S., Cheng, M., Pu, C., . . . Liu, C. (2022). Association between microRNA-146a rs2910164 polymorphism and coronary heart disease: An updated meta-analysis. *Medicine, 101*(46).

Campbell, F. M., Kozak, R., Wagner, A., Altarejos, J. Y., Dyck, J. R., Belke, D. D., . . . Lopaschuk, G. D. (2002). A role for peroxisome proliferator-activated receptor α (PPARα) in the control of cardiac malonyl-CoA levels: reduced fatty acid oxidation rates and increased glucose oxidation rates in the hearts of mice lacking PPARα are associated with higher concentrations of malonyl-CoA and reduced expression of malonyl-CoA decarboxylase. *Journal of Biological Chemistry, 277*(6), 4098-4103.

Cardoso, A. C., Lam, N. T., Savla, J. J., Nakada, Y., Pereira, A. H. M., Elnwasany, A., . . . Sharma, G. (2020). Mitochondrial substrate utilization regulates cardiomyocyte cell-cycle progression. *Nature metabolism, 2*(2), 167-178.

Cheng, Y., Liu, X., Zhang, S., Lin, Y., Yang, J., & Zhang, C. (2009). MicroRNA-21 protects against the H2O2-induced injury on cardiac myocytes via its target gene PDCD4. *Journal of molecular and cellular cardiology, 47*(1), 5-14.

Cosmi, F., Shen, L., Magnoli, M., Abraham, W. T., Anand, I. S., Cleland, J. G., . . . Dickstein, K. (2018). Treatment with insulin is associated with worse outcome in patients with chronic heart failure and diabetes. *European journal of heart failure, 20*(5), 888-895.

Das, S., Ferlito, M., Kent, O. A., Fox-Talbot, K., Wang, R., Liu, D., . . . Murphy, E. (2012). Nuclear miRNA regulates the mitochondrial genome in the heart. *Circulation research, 110*(12), 1596-1603.

Dillmann, W. H. (2019). Diabetic cardiomyopathy: what is it and can it Be Fixed? *Circulation research, 124*(8), 1160-1162.

Emad, H. (2018). Stem Cell Therapy for Vascular Disorders. *Vascular & Endovascular Review, 1*.

Fukushima, A., & Lopaschuk, G. D. (2016). Cardiac fatty acid oxidation in heart failure associated with obesity and diabetes. *Biochimica et Biophysica Acta (BBA)-Molecular and Cell Biology of Lipids, 1861*(10), 1525-1534.

Gong, H., Chen, H., Xiao, P., Huang, N., Han, X., Zhang, J., . . . Tai, H. (2022).

miR-146a impedes the anti-aging effect of AMPK via NAMPT suppression and NAD+/SIRT inactivation. *Signal Transduction and Targeted Therapy, 7*(1), 66.

Guo, R., & Nair, S. (2017). Role of microRNA in diabetic cardiomyopathy: from mechanism to intervention. *Biochimica et biophysica acta (BBA)-molecular basis of disease, 1863*(8), 2070-2077.

Haemmerle, G., Moustafa, T., Woelkart, G., Büttner, S., Schmidt, A., Van De Weijer, T., . . . Zierler, K. (2011). ATGL-mediated fat catabolism regulates cardiac mitochondrial function via PPAR-α and PGC-1. *Nature medicine, 17*(9), 1076-1085.

Harada, M., Luo, X., Murohara, T., Yang, B., Dobrev, D., & Nattel, S. (2014). MicroRNA regulation and cardiac calcium signaling: role in cardiac disease and therapeutic potential. *Circulation research, 114*(4), 689-705.

Hashimoto, T., Cook, W. S., Qi, C., Yeldandi, A. V., Reddy, J. K., & Rao, M. S. (2000). Defect in peroxisome proliferator-activated receptor α-inducible fatty acid oxidation determines the severity of hepatic steatosis in response to fasting. *Journal of Biological Chemistry, 275*(37), 28918-28928.

He, J., Lu, Y., Song, X., Gong, X., & Li, Y. (2019). Inhibition of microRNA-146a attenuated heart failure in myocardial infarction rats. *Bioscience reports, 39*(12), BSR20191732.

Jaquenod De Giusti, C., Palomeque, J., & Mattiazzi, A. (2022). Ca2+ mishandling and mitochondrial dysfunction: a converging road to prediabetic and diabetic cardiomyopathy. *Pflügers Archiv-European Journal of Physiology, 474*(1), 33-61.

Jia, G., Hill, M. A., & Sowers, J. R. (2018). Diabetic cardiomyopathy: an update of mechanisms contributing to this clinical entity. *Circulation research, 122*(4), 624-638.

Jia, G., Whaley-Connell, A., & Sowers, J. R. (2018). Diabetic cardiomyopathy: a hyperglycaemia-and insulin-resistance-induced heart disease. *Diabetologia, 61*(1), 21-28.

Kannel, W. B., Hjortland, M., & Castelli, W. P. (1974). Role of diabetes in congestive heart failure: the Framingham study. *The American journal of cardiology, 34*(1), 29-34.

Li, H., Fan, J., Chen, C., & Wang, D. W. (2020). Subcellular microRNAs in diabetic cardiomyopathy. *Annals of Translational Medicine, 8*(23).

Louch, W. E., Sheehan, K. A., & Wolska, B. M. (2011). Methods in cardiomyocyte isolation, culture, and gene transfer. *Journal of molecular and cellular cardiology, 51*(3), 288-298.

Luo, L., Yan, C., Fuchi, N., Kodama, Y., Zhang, X., Shinji, G., . . . Li, T.-S. (2021). Mesenchymal stem cell-derived extracellular vesicles as probable triggers of radiation-induced heart disease. *Stem cell research & therapy, 12*(1), 1-13.

Luptak, I., Balschi, J. A., Xing, Y., Leone, T. C., Kelly, D. P., & Tian, R. (2005). Decreased contractile and metabolic reserve in peroxisome proliferator–activated receptor-α–null hearts can be rescued by increasing glucose transport and utilization. *Circulation, 112*(15), 2339-2346.

Madrazo, J. A., & Kelly, D. P. (2008). The PPAR trio: regulators of myocardial energy metabolism in health and disease. *Journal of molecular and cellular cardiology, 44*(6), 968-975.

Melman, Y. F., Shah, R., & Das, S. (2014). MicroRNAs in heart failure: is the picture becoming less miRky? *Circulation: Heart Failure, 7*(1), 203-214.

Milano, G., Biemmi, V., Lazzarini, E., Balbi, C., Ciullo, A., Bolis, S., . . . Barile, L. (2020). Intravenous administration of cardiac progenitor cell-derived exosomes protects against doxorubicin/trastuzumab-induced cardiac toxicity. *Cardiovascular Research, 116*(2), 383-392.

Montaigne, D., Marechal, X., Coisne, A., Debry, N., Modine, T., Fayad, G., . . . Sebti, Y. (2014). Myocardial contractile dysfunction is associated with impaired mitochondrial function and dynamics in type 2 diabetic but not in obese patients. *Circulation, 130*(7), 554-564.

Pan, J.-A., Tang, Y., Yu, J.-Y., Zhang, H., Zhang, J.-F., Wang, C.-Q., & Gu, J. (2019). miR-146a attenuates apoptosis and modulates autophagy by targeting TAF9b/P53 pathway in doxorubicin-induced cardiotoxicity. *Cell Death & Disease, 10*(9), 668.

Patro, R., Duggal, G., Love, M. I., Irizarry, R. A., & Kingsford, C. (2017). Salmon provides fast and bias-aware quantification of transcript expression. *Nature methods, 14*(4), 417-419.

Pol, C. J., Lieu, M., & Drosatos, K. (2015). PPARs: protectors or opponents of myocardial function? *PPAR research, 2015*.

Rydén, L., Armstrong, P., Cleland, J., Horowitz, J., Massie, B., Packer, M., & Poole-Wilson, P. (2000). Efficacy and safety of high-dose lisinopril in chronic heart failure patients at high cardiovascular risk, including those with diabetes mellitus. Results from the ATLAS trial. *European heart journal, 21*(23), 1967-1978.

Scărlătescu, A. I., Barbălată, T., Sima, A. V., Stancu, C., Niculescu, L. Ș., & Micheu, M. M. (2022). miR-146a-5p, miR-223-3p and miR-142-3p as Potential Predictors of Major Adverse Cardiac Events in Young Patients with Acute ST Elevation Myocardial Infarction—Added Value over Left Ventricular Myocardial Work Indices. *Diagnostics, 12*(8), 1946.

Shah, R., Ziegler, O., Yeri, A., Liu, X., Murthy, V., Rabideau, D., . . . Tackett, M. (2018). MicroRNAs associated with reverse left ventricular remodeling in humans identify pathways of heart failure progression. *Circulation: Heart Failure, 11*(2), e004278.

Shen, L., Li, C., Zhang, H., Qiu, S., Fu, T., & Xu, Y. (2019). Downregulation of miR-146a contributes to cardiac dysfunction induced by the tyrosine kinase inhibitor sunitinib. *Frontiers in Pharmacology, 10*, 914.

Shindler, D. M., Kostis, J. B., Yusuf, S., Quinones, M. A., Pitt, B., Stewart, D., . . . investigators, S. (1996). Diabetes mellitus, a predictor of morbidity and mortality in the Studies of Left Ventricular Dysfunction (SOLVD) Trials and Registry. *The American journal of cardiology, 77*(11), 1017-1020.

Su, Q., Xu, Y., Cai, R., Dai, R., Yang, X., Liu, Y., & Kong, B. (2021). miR-146a inhibits mitochondrial dysfunction and myocardial infarction by targeting cyclophilin D. *Molecular Therapy-Nucleic Acids, 23*, 1258-1271.

Wang, S., Lv, T., Chen, Q., Yang, Y., Xu, L., Zhang, X., . . . Liu, Y. (2022). Transcriptome sequencing and lncRNA-miRNA-mRNA network construction in cardiac fibrosis and heart failure. *Bioengineered, 13*(3), 7118-7133.

Watanabe, K., Fujii, H., Takahashi, T., Kodama, M., Aizawa, Y., Ohta, Y., . . . Nakajima, T. (2000). Constitutive regulation of cardiac fatty acid metabolism through peroxisome proliferator-activated receptor α associated with age-dependent cardiac toxicity. *Journal of Biological Chemistry, 275*(29), 22293-22299.

Wong, L. L., Wang, J., Liew, O. W., Richards, A. M., & Chen, Y.-T. (2016). MicroRNA and heart failure. *International journal of molecular sciences, 17*(4), 502.

Xiong, Y., Tang, R., Xu, J., Jiang, W., Gong, Z., Zhang, L., . . . Chen, G. (2022). Tongxinluo-pretreated mesenchymal stem cells facilitate cardiac repair via exosomal transfer of miR-146a-5p targeting IRAK1/NF-κB p65 pathway. *Stem cell research & therapy, 13*(1), 289.

Xu, J., Xiao, G., Trujillo, C., Chang, V., Blanco, L., Joseph, S. B., . . . Lee, W. P. (2002). Peroxisome proliferator-activated receptor α (PPARα) influences substrate utilization for hepatic glucose production. *Journal of Biological Chemistry, 277*(52), 50237-50244.

Zhang, Y., Su, W., Zhang, Q., Xu, J., Liu, H., Luo, J., . . . Lei, S. (2018). Glycine protects H9C2 cardiomyocytes from high glucose-and hypoxia/reoxygenation-induced injury via inhibiting PKCβ2 activation and improving mitochondrial quality. *Journal of diabetes research, 2018*.

Zou, T., Zhu, M., Ma, Y.-C., Xiao, F., Yu, X., Xu, L., . . . Dong, J.-Z. (2018). MicroRNA-410-5p exacerbates high-fat diet-induced cardiac remodeling in mice in an endocrine fashion. *Scientific Reports, 8*(1), 8780.